

Effects of Undulator Errors on Beam Motion*

R. K. Koul

Argonne National Laboratory, 9700 Cass Ave., Argonne, IL 60439

Abstract

At the Advanced Photon Source (APS) it is planned to have an undulator test line for measuring the field quality of the undulators. The effect of both uncorrelated and correlated errors is evaluated. The effect of errors is shown to fall inversely proportional to gamma. The effect of the correlated errors is found to be smaller by factor of approximately the average value of the correlation function over one-half a wavelength.

1 INTRODUCTION

At the Advanced Photon Source an undulator test line is proposed for measuring the field quality of the undulators. These undulators will be used eventually in straight sections of the storage ring. The test line diverts the electrons or positrons from the PTB transport line which carries beam from the positron accumulator ring to the injector synchrotron. While the energy of the storage ring electrons will be 7 GeV, the energy at the test line will be about 450 MeV. The questions one may ask are: (1) What is the effect of undulator errors on the beam as it moves through the undulator, and (2) How does this affect scale with the energy of the beam? A related question would be (3) Can these undulators be used as diagnostic tool for the beam at high energy?

In order to answer the first question one has to ask about the type of errors one may expect in the undulators. It is commonly understood that the undulator errors get correlated because of the interaction with adjoining poles. However, the exact nature of the correlation is not clear. For planar undulators one expects the correlation to be given by $\sin kz$ [1]. Therefore, for our undulator type A, which is three-dimensional in character, we have used three different types of errors for the numerical study. These are (1) purely random field errors, say δB_y , attached to each pole, (2) errors of the type $\delta B_y \sin kz$, where δB_y is again the random error at each pole and $\sin kz$ gives the correlation of errors, and finally (3) the coefficient B_0 of the solution of the three-dimensional undulator is modified as $B_0 + \delta B_0$. The form of the equations of motion through the undulator with these errors is discussed in the section on numerical simulation.

The analytic method discussion in the second section starts with the Hamiltonian [2][3] associated with the motion of the electrons in an undulator. The analytic calcu-

lations have been carried out using random errors at each pole. The comparison with the numerical results of the same case are found to be in excellent agreement.

In the end we discuss the results of the numerical simulation of the three cases mentioned above and compare the results, in the case of the random errors, with analytical results.

2 ANALYTICAL METHOD

Let $\{x, y, z\}$ be the standard rectangular coordinates associated locally with the undulator magnet. Here z is along the length, y along the vertical direction, and x along the horizontal direction. The magnetic field in a undulator has been characterized by vector potential (A_x, A_y) [2][4]. The vector potential characterizing the three-dimensional undulator magnetic field in Cartesian coordinates is given by,

$$A_x = -\frac{B_0}{k} \cosh(k_x x) \cosh(k_y y) \sin kz, \quad (1)$$

$$A_y = \frac{k_x}{k k_y} B_0 \sinh(k_x x) \sinh(k_y y) \sin kz. \quad (2)$$

In Eq.(1) and Eq.(2) we have $k^2 = k_x^2 + k_y^2$ and also $k = 2\pi/l$, where l is the cell length. Let P_0 be the initial energy, m the mass, $\beta = \sqrt{1-1/\gamma^2}$, with γ as the relativistic factor. Furthermore let $P_x = (p_x + eA_x)$ and $P_y = (p_y + eA_y)$ be the canonical momenta in the x and y directions with p_x and p_y the kinematic momenta. With these definitions we can write the Lloyd Smith Hamiltonian H [2]. Next we carry out a sequence of canonical transformations similar to the ones suggested in [2] and transform to coordinates $\{\chi, y, s\}$. Now $x = x_e + z'_e \chi$, $z = z_e - x'_e \chi$, $P_x = z'_e P_\chi + \frac{x'_e}{(1+\Omega\chi)} P_s$, $P_z = -x'_e P_\chi + \frac{z'_e}{(1+\Omega\chi)} P_s$, $y = y$, and $P_y = P_y$. We furthermore expand the hyperbolic functions as power series and finally write the Hamiltonian to the second order. In this approximation the Hamiltonian H can be written as

$$H = \frac{1}{2p_0} [P_\chi^2 + P_y^2] + \frac{p_0}{\rho} \chi \cos kz_e + \frac{p_0 \sin kz_e^2}{2k^2 \rho^2} [k_x^2 \chi^2 + k_y^2 y^2]. \quad (3)$$

In Eq. (3) energy can be expressed as $cP_0 = mc^2/\sqrt{1-\beta^2}$ and $eB_0\rho = p_0$.

Next consider the random dipole type errors of integrated strength $\frac{\delta B}{B_0} l$, centered at the pole of the undulator,

*Work supported by U. S. Department of Energy, Office of Basic Energy Sciences under Contract No. W-31-109-ENG-38.

where $l = \frac{\lambda}{2}$ is the half wavelength. Under these assumptions it is straightforward to show that for a single error at the i^{th} pole the momentum change is given by

$$\Delta p_x = \frac{p_0}{\rho} \frac{\delta B(z_i)}{B_0} l. \quad (4)$$

Note that $\Delta p_x = mc\beta\gamma\delta\chi'$. Integrating Eq.(4) with the substitution for Δp_x gives the contribution from a single error. The contribution from random errors at different poles is the sum of the contribution from each pole. Thus calling $\Delta\chi$ the total change we have,

$$\Delta\chi = -\frac{\lambda}{2\rho} \sum_{i=0}^{i=n} \frac{\delta B(z_i)}{B_0} (L - z_i). \quad (5)$$

In the above equation L is the length of the undulator, z_i is the position of the i^{th} pole of the undulator, and $\Delta\chi$ will be the total displacement at the end of the undulator. Thus we see that the effect of the undulator errors is inversely proportional to γ . For details about the above results, see [5].

3 NUMERICAL SIMULATION

The numerical simulation was carried out using the exact equations of motion and writing a program using MathematicaTM. There are three coupled set of equations with a mass constraint. We used the mass constraint to obtain an expression for $\frac{\beta'_z}{\beta}$, where β' refers to the derivative of β with respect to z . We can write the equations as

$$x'' + \frac{\beta'_z}{\beta_z} x' = \frac{e}{\beta_z p_0} [-B_y + y' B_z] \quad (6)$$

$$y'' + \frac{\beta'_z}{\beta_z} y' = \frac{e}{\beta_z p_0} [-B_x + x' B_z] \quad (7)$$

$$\beta_z^2 = \beta^2 - \beta_x^2 - \beta_y^2. \quad (8)$$

Note that $\beta = \sqrt{1 - \gamma^{-2}}$ is a constant of the equations of motion. Differentiating Eq.(8) and using Eq.(6) and Eq.(7), we can eliminate the term $\frac{\beta'_z}{\beta_z}$ from Eq.(6) and Eq.(7). Then we obtain a coupled set of linear differential equations with variables x and y with independent parameter z . We solved these equations numerically, using MathematicaTM.

Three types of errors were studied. The first one was the completely random error in B_y . On the right-hand side of Eq.(6) $-B_y$ is replaced by $-B_y + \delta B_y$, where δB_y is randomly chosen at each pole. The second type of error, similar to one introduced by [1], changes B_y to $B_y + \delta B_y \cos kz$. The third type of error is introduced by changing the coefficient B_0 of the vector potential (A_x, A_y) to $B_0 + \delta B_0$. The effective vector potential satisfies the boundary conditions of the problem and is a very close solution. In this type of error the components B_x, B_y and B_z change, and term δB_0 is again chosen randomly at each pole.

Equations (6) through (8) were solved first without errors and later with errors.

4 RESULTS

The simulation was carried out for APS undulator type A, for which $\lambda = 0.033\text{m}$, $k_x = 126.0\text{m}^{-1}$, $k_y = 142.744\text{m}^{-1}$, $B_0 = .807509\text{ T}$, and the undulator length is 2.477 meters. The initial conditions for all the runs were $x = y = x' = y' = 0$. The energy was varied from 500 MeV to 7.5 GeV. The simulation carried out for the undulator without errors gave 0.8 microns displacement at 500 MeV of energy. This displacement varies inversely with the energy. Figures 1 through 6 show the results of the analytical calculations and the numerical simulations. Figures 1, 2, 3, and 6 plot displacement, in meters, as a function of energy given in terms of γ . The energy value 1 on the plot corresponds to 500 MeV, with increments of 500 MeV. Figure 5 plots the vertical displacement in meters, as a function of energy.

In order to compare the analytical and numerical results, several sets of random errors with rms values lying in the range of .005 to .007 were generated. The horizontal displacement values at the end of the undulator were calculated using both the methods. In each case the comparison was exact. The horizontal, i.e., x , displacement at the end of undulator varies inversely with the energy of the particle (see Fig. 2). This is what the analytical expression in Eq.(5) states and what can be seen in Fig. 1. The mean of the absolute values of the displacements, for ten simulations, was 500 microns for the mean random errors value of .006, at an energy of 500 MeV. Thus, the mean at other energies was $500/\gamma$.

Figure 3 is a typical plot of the random errors chosen for the δB_0 . Figure 4 is also a plot of horizontal displacement as function of energy at the end of the undulator for errors of type 2, i.e., errors in which B_y was replaced by $B_y + \delta B_y \cos kz$. In this case again the displacement is inversely proportional to energy, but the displacement at 500 MeV is only about 3.5 microns. Similarly for error type 3, described earlier, the magnitude of displacement varies from one to five microns at 500 MeV. Again displacement falls inversely with energy. In such a situation these displacements will not be measurable. There is no displacement along the y -direction in all these cases, as one can see from Fig. 5.

5 REFERENCES

- [1] Brian M. Kincaid, "RANDOM ERRORS IN UNDULATORS AND THEIR EFFECTS ON THE RADIATION SPECTRUM," Nuclear Instruments and Methods in Physics Research, A26, pp.109-119 (1986).
- [2] Lloyd Smith, "EFFECT OF WIGGLERS AND UNDULATORS ON BEAM DYNAMICS," ESG Tech Note-24, 1986.
- [3] R. K. Koul, "Methods Of Hamiltonian Vector Fields and Phase Space," to be published.
- [4] K. Halbach, "Physical and Optical Properties of Rare Earth Cobalt Magnets," Nuclear Instruments and Methods, 187, pp.109-117, 1981.
- [5] R. K. Koul, to be published.

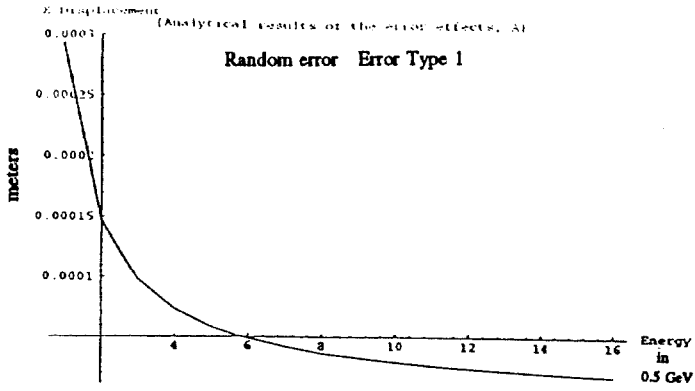


Figure 1

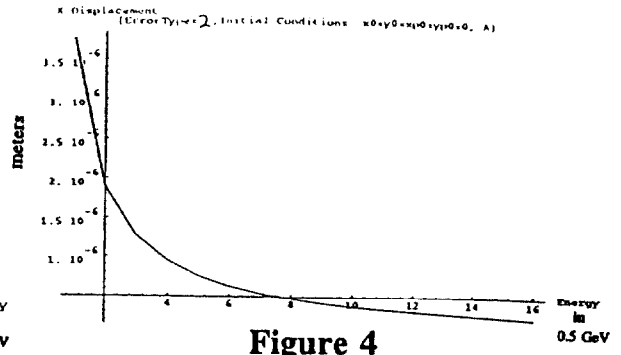


Figure 4

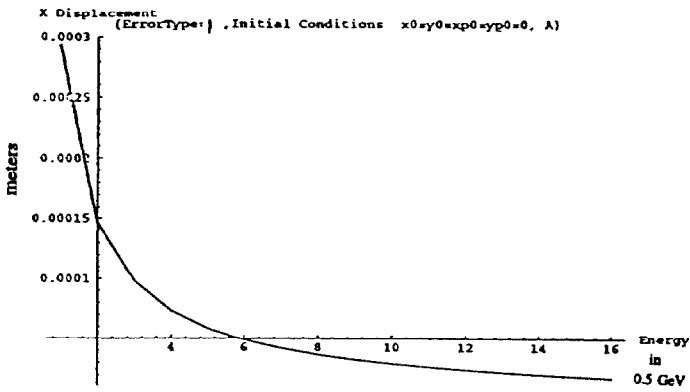


Figure 2

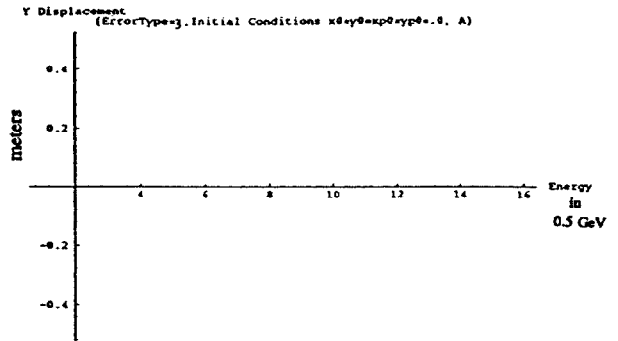


Figure 5

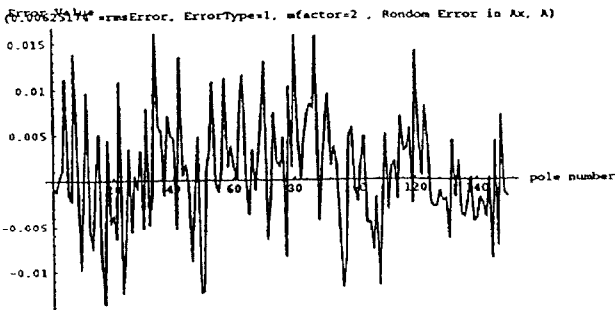


Figure 3

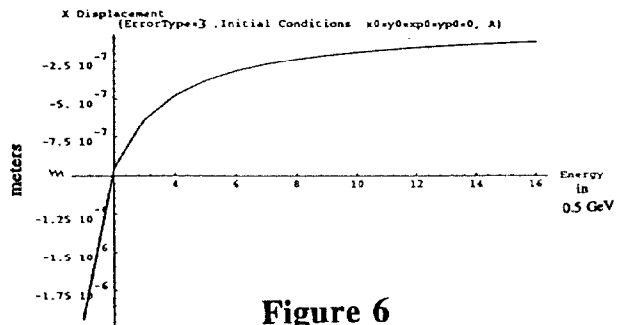


Figure 6